RSC Advances

PAPER

View Article Online
View Journal | View Issue

Cite this: *RSC Adv.*, 2021, **11**, 29807

Highly selective enrichment of Au using enaminone covalent organic polymers (COP)

An Li, Naixia Zheng, Tao Yang, Jun Xie, LiJun Li, KeWen Tang * and CongShan Zhou *

Received 18th May 2021
Accepted 29th July 2021

DOI: 10.1039/d1ra03868k

rsc.li/rsc-advances

The second recovery of gold has fundamental environmental and economic significance. In this study, an enaminone covalent organic polymer (COP) was synthesized and used to recover gold from secondary resources. The ketene covalent organic polymer (COP) possessed good gold adsorption performance, and the best adsorption capacity could reach up to 1945 mg g^{-1} at 298 K, which was superior to traditional adsorbents. Meanwhile, the synthesized COP exhibited excellent adsorption selectivity and renewability of Au^{3+}. The pseudo-second-order kinetic equation and Langmuir equation were suggested for describing the adsorption process. Moreover, this gold adsorption behavior was intended to be a spontaneous, endothermic, and entropy increasing process.

1. Introduction

Gold (Au) is a precious metal and widely utilized in numerous fields, including catalysis,[1–3] biomedicine,[4,5] analytical chemistry[6] and photoelectricity.[7,8] In various fields, it will inevitably be lost to the solution and mixed with other metals, resulting in a waste of resources and environmental pollution. Therefore, the recycling of Au has become an economic and ecological problem worthy of attention.[9] Adsorption is considered as the most promising method for Au recycling because of its simple operation and high efficiency as well as low cost.[10–12] However, it is urgent to develop novel adsorbents with a large adsorption capacity, excellent selectivity and fast adsorption speed for Au.[12]

Recently, recycling Au has been attracting more and more attention. Activated carbon[13,14] is usually employed as adsorbent to enrich Au from the recovered solution due to its abundant pore structure, easy elution, and environmental friendliness. However, the rate of repeated elution and reactivation reduces the activity of activated carbon, leading to the decreasing of the recovery of gold.[15] Resin[16,17] is also utilized as high-effective adsorbent to recover many metals. Although the resins present the merit of high loading capacity, fast adsorption rate, and low transparency of the solution, the selectivity for recycling Au is really low. The resins are easy to be interfered with by other ions in the adsorption process, which leads to the increase of resin demand, and the production cost of resin is relatively high.[16] Besides, MOFs are regarded as a kind of promising adsorbents with the advantages of regular pore structure, adjustable functional groups, high specific surface area as well as good stability. Whereas the adsorption capacity of gold ion over MOFs is limited and needed to be addressed.[18,19] Therefore, the further development of novel adsorbents for recycling Au from secondary resources with high adsorption capacity as well as excellent selectivity is still highly desired.

In this paper, a novel covalent organic polymer was synthesized successfully using ketene monomer and amine as the monomers. The synthesized ketene COP possessed plentiful pore structure as well as uniform pore size distribution. Furthermore, the adsorptive property of COP was studied to enrich Au from aqueous solutions. The kinetics, isotherm, thermodynamics and adsorption mechanism were systematically investigated.

2. Experimental section

2.1. Materials and instrumentation

All reagents and materials were analytic purity and supplied by Sinopharm Chemical Reagent Company. Fourier transform infrared spectrometer (FT-IR), Brunauer–Emmett–Teller (BET), thermogravimetry differential scanning calorimetry (TG-DSC), scanning electron microscope (SEM, Zeiss, 3 kV), powder X-ray diffraction (PXRD), transmission electron microscopy (TEM), and X-ray photoelectron spectroscopy (XPS). The concentration of Au(III) determines by an atomic absorption spectrometer (Shimadzu AA-6880).

2.2. Synthesis of COP

Triphenyl-dimethylamino propenone (2 eq.), *p*-phenylenediamine (3 eq.), measure the methanol (4 mL) and acetic acid (1 mL) were mixed and dissolved in the reaction tube. Then, the mixture solution was sealed and reacted for 4 days under strong stirring at room temperature. After reaction finished, the generated solid product was separated *via* centrifugation, washed with ethanol and then dried in drying oven.

Province Key Laboratory for Fine Petrochemical Catalysis and Separation, College of Chemistry and Chemical Engineering, Hunan Institute of Science and Technology, Yueyang, Hunan, 414000, P. R. China. E-mail: tangkewen@sina.com; zhoucongsh@126.com

2.3. Adsorption experiment

The adsorption property of Au ion was tested *via* batch adsorption experiments. Firstly, $(AuCl_4)^-$ was obtained *via* the dissolving of gold nugget in aqua regia. For each adsorption test, 10 mg of adsorbent material was shaken with 10 mL of Au^{3+} solution into 50 mL centrifuge tube at 280 rpm. The pH value of the solution was adjusted *via* sodium hydroxide or dilute hydrochloric acid solution. In the adsorption kinetics experiments, the material was treated with 3000 ppm Au^{3+} solution at 298 K for 24 hours to study the adsorption kinetics. The adsorption isotherms and thermodynamics were studied at 278K–318 K. The initial concentration of Au was between 100 ppm and 5000 ppm. Meanwhile, adsorption capacity of metal ion was calculated as follows:

$$Q_e = \frac{(C_0 - C_e)V}{m} \quad (1)$$

$$Q_t = \frac{(C_0 - C_t)V}{m} \quad (2)$$

Q_e (mg g^{-1}) and Q_t (mg g^{-1}) respectively represented the adsorption capacity at equilibrium and corresponding adsorption time t (h). C_0 (mg g^{-1}) and C_t (mg g^{-1}) were the initial concentration and the concentration after adsorption; C_e (mg g^{-1}) was the adsorption concentration reaching equilibrium. V (L) was the solution volume, m (g) was the weight of adsorbent material.

The pseudo-first-order and pseudo-second-order dynamic models were used to analyze the dynamic results.[20] The formulas of the two models were as follows:

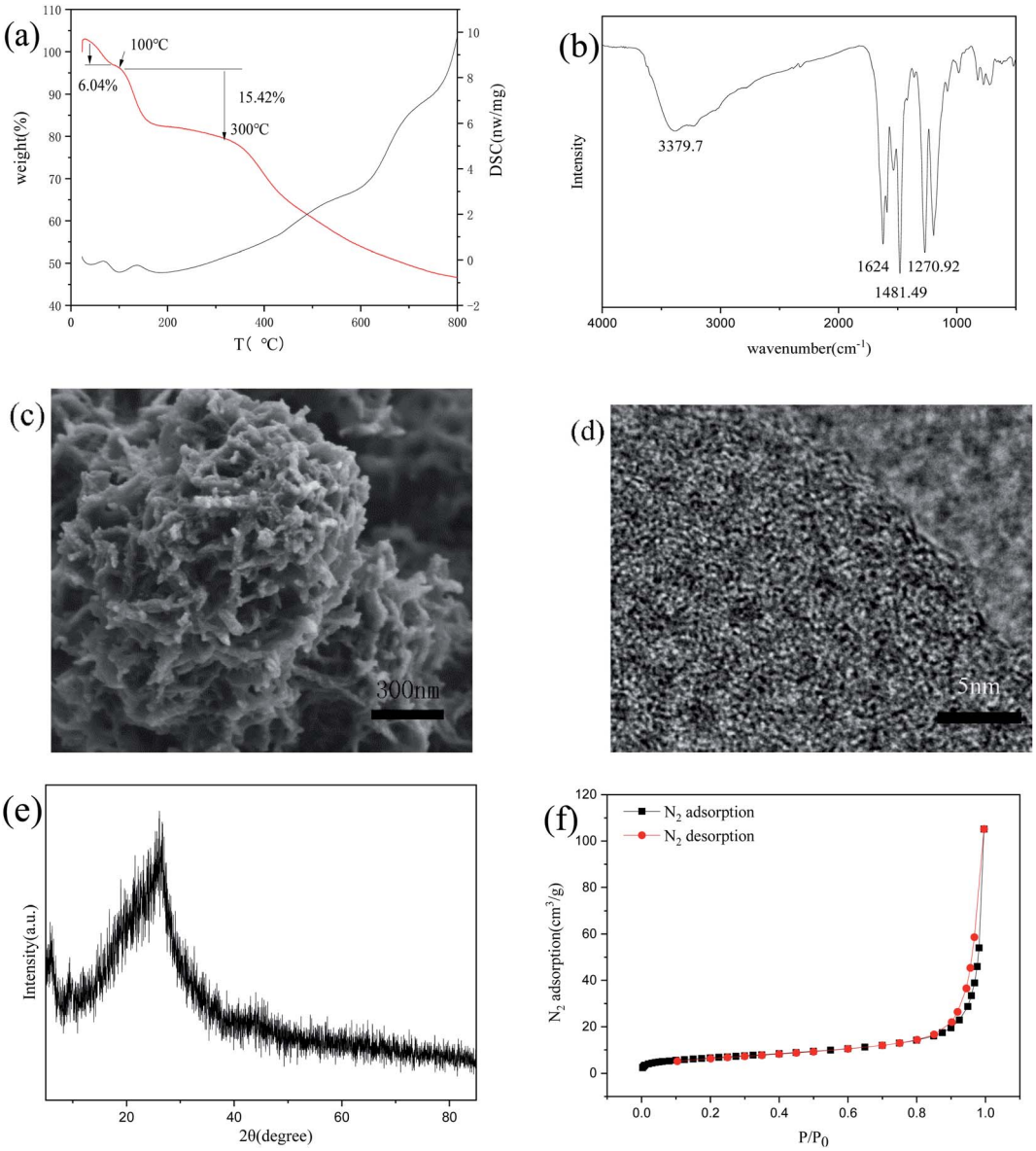

Fig. 1 The structure characterization of the synthesized COP. (a) TG-DSC spectra; (b) FTIR spectra; (c) SEM picture; (d) TEM image; (e) PXRD image; (f) N_2 adsorption–desorption isotherms.

$$\ln(Q_e - Q_t) = -k_1 t + \ln Q_e \quad (3)$$

$$\frac{t}{Q_t} = \frac{t}{Q_e} + \frac{1}{k_2 \times Q_e^2} \quad (4)$$

k_1 (h^{-1}) and k_2 (g mg^{-1} h^{-1}) represented the rate constant of pseudo-first-order and the rate constant of pseudo-second-order.

Both Langmuir and Freundlich adsorption models were employed to fit the temperature with the adsorption Au^{3+} data of COP.[10] The equation definition of each adsorption isotherm is as follows:

$$Q_e = \frac{K_L \times Q_m \times C_e}{1 + K_L \times C_e} \quad (5)$$

$$Q_e = K_F \times C_e^{1/n_F} \quad (6)$$

Q_m (mg g^{-1}) was the maximum adsorption capacity of Au^{3+}, K_L (L mg^{-1}) was the adsorption constant of Langmuir isotherm, and n_F and K_F are the adsorption constants of Freundlich isotherm.

3. Results and discussion

3.1. Structural characterization

The COP is successfully prepared by the one-pot method, which is simple and straightforward to obtain the final adsorbents. The structure of COP characterizes by TG-DSC, PXRD, BET, SEM, TEM, XPS, and FT-IR, and the characteristic results are shown as follows. As shown in Fig. 1a, thermogravimetric analysis shows that the loss of adsorbed water causes 6.04% of the weight loss below 100 °C. When the material slowly decreases from 100 °C to 300 °C, the material's weight loss is 15.42%, caused by the pore size's collapse outside the material. The weight of COP material decreases slowly after 300 °C due to the decomposition of volatile organic components. From the infrared spectrum in Fig. 1b, one can see that the NH tensile vibration peak at 3379.7 cm^{-1} is observed obviously.[15,20] There is a C=O tensile vibration peak at 1624 cm^{-1}.[21,22] There is C=C tensile vibration at 1481.49 cm^{-1}. There is a C–N tensile vibration peak at 1270.92 cm^{-1}.[21] SEM and TEM characterize the morphology of COP. The SEM images in Fig. 1c show that the material has a fluffy network structure. TEM images in Fig. 1d further verify the uniformity of the material structure. The high-resolution TEM images confirm that the material is amorphous, consonant with PXRD results shown in Fig. 1e. The inset of Fig. 1f shows that the specific surface area is 23.9617 m^2 g^{-1}, indicating that it is a macroporous polymer.

3.2. Adsorption behavior study

3.2.1. The effect of pH for Au^{3+} adsorption. Generally, the pH of solution has significant effect on the adsorption of metal ions, because pH can change the surface charge and metal ions which alters the interaction between adsorbents with metal ions. The effect of pH for the adsorption of Au^{3+} over COP adsorbents was studied in different pH solution environments. As shown in Fig. 2, with the increasing the pH of solution, the adsorption capacity Au^{3+} over COP adsorbents decreases sharply. As a result, the COP adsorbent exhibits outstanding achievement under acidic conditions for the adsorption of Au^{3+} ions.

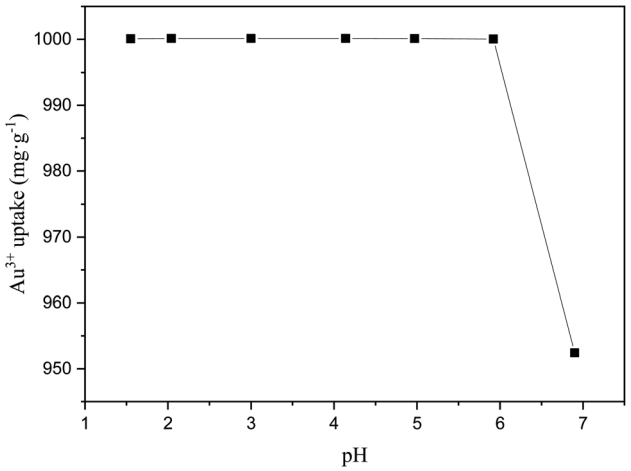

Fig. 2 The influence of pH for adsorbing Au^{3+} over COP. Condition: temperature: 298 K; adsorption time: 24 h; material: 10 mg; volume: 10 mL; concentration of Au^{3+}: 1000 mg L^{-1}.

3.2.2. Adsorption kinetics study. As shown in Fig. 3, the association between adsorption time and adsorption quantity of Au^{3+} is investigated. The pseudo-first-order kinetics (eqn (3)) as well as pseudo-second-order kinetics (eqn (4)) are respectively fitted to further study adsorption kinetics for the adsorption behavior of Au^{3+} over COP adsorbent. The reliability of the model is evaluated by determining the corresponding value of coefficient R^2. Generally, the higher R^2, the closer the actual value of Au^{3+} absorption is to the theoretical value. Obviously, the R^2 value (0.998) of pseudo-second-order kinetic model is higher than that (0.856) of pseudo-first-order kinetic model, as shown in Table 1. This result indicates that the pseudo-second-order kinetic model is suited to the adsorption dynamics of Au^{3+} over the COP adsorbent.

3.2.3. Study of adsorption isotherms and thermodynamics. Under adsorption conditions of pH is 2.5, the adsorbent dosage is 10 mg, initial concentration of metal ion is 100–5000 ppm,

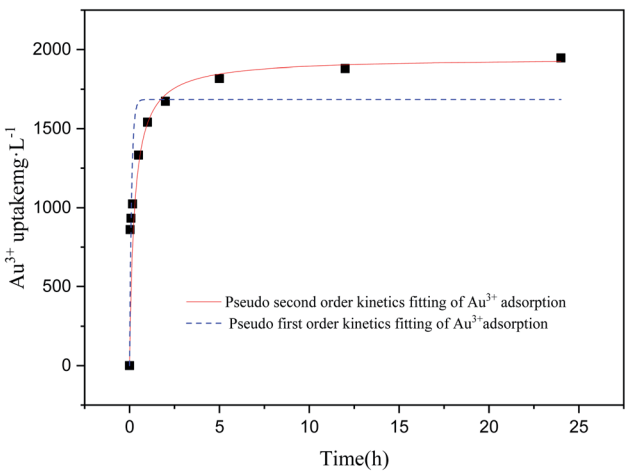

Fig. 3 The influence of time for adsorbing Au^{3+} over COP. Condition: temperature: 298 K; pH of solution: 2.5; material: 10 mg; volume: 10 mL; concentration of Au^{3+}: 3000 mg L^{-1}.

Table 1 The kinetics parameters of adsorbing Au^{3+} over COP

	Pseudo-first order			Pseudo-second order		
C_0 (mg L^{-1})	Q_e (mg g^{-1})	k_1 (min^{-1})	R^2	Q_e (mg g^{-1})	k_2 (g mg^{-1} min^{-1})	R^2
3000	792.66	0.0027	0.8564	1945.52	0.0000245	0.9982

and adsorption equilibrium time is 24 hours, adsorption isotherms of COP for Au^{3+} are detailedly studied. The adsorption isotherms show similar shapes at different temperatures. As the increase of equilibrium concentration of Au^{3+}, the adsorption capacity for Au^{3+} increases rapidly and then increases lowly. When equilibrium concentration of Au^{3+} reaches to critical value, which is the stable value. Meanwhile, the Langmuir equation (eqn (5)) and Freundlich (eqn (6)) adsorption model are used for adsorption isotherm data of Au^{3+}, and the modeling results as well as corresponding parameters are summarized in Fig. 4 and Table 2. Apparently, the Langmuir adsorption model is better for describing the adsorption performance of COP to Au^{3+} than the Freundlich model. The theoretical value of the Langmuir model is nearer to the test data of adsorption capacity of Au^{3+}, relative to that of the Freundlich one. Therefore, the Langmuir adsorption model is more proper to explain the adsorption isotherm of Au^{3+} by COP.

The synthesized COP is a promising adsorbent material for adsorbing Au(III) from water. According to the Van Kerkhoff equation (eqn (7)), the Gibbs free energy (ΔG) equation is as follows:

$$\Delta G = -RT \ln K_e \quad (7)$$

R represents the constant of an ideal gas (8.314 J mol^{-1} K^{-1}), T (K) represents adsorption temperature, and K_e represents thermodynamic equilibrium constant. It is suggested that K_e is dimensionless and can be accomplished *via* converting the section of the given adsorption fixed (kg) in the following ways:[23]

Table 2 Isotherm parameters of adsorbing Au^{3+} over COP

	Freundlich			Langmuir		
T (K)	K_F	N	R^2	K_L (L mg^{-1})	q_m (mg g^{-1})	R^2
278	400.49	5.98	0.8519	0.01	1539.92	0.8552
298	1143.97	14.49	0.6580	0.04	1937.83	0.9819
308	1476.83	19.66	0.5898	0.07	2162.61	0.9198
318	1846.70	29.88	0.5046	0.14	2363.08	0.9231

$$K_e = \frac{1000 \times K_G \times M_{adsorbate} \times [adsorbate]^0}{\gamma} \quad (8)$$

where $M_{adsorbate}$ (g mol^{-1}) represents the adsorbed ion's molecular weight, $[adsorbate]^0$ represents the standard concentration of adsorbate, and γ represents the assumed activity coefficient of 1. According to the third law of thermodynamics, the connection between K_e and enthalpy change (ΔH_0) and entropy change (ΔS) is as follows:

$$\ln K_e = \frac{\Delta S}{R} - \frac{\Delta H}{RT} \quad (9)$$

As shown in Fig. 5, ΔS and ΔH can obtain from the linear curve of ln K_e. Table 3 directly shows all the thermodynamic parameters. The value of ΔG at each temperature is negative, implying the spontaneity and feasibility for adsorbing Au^{3+} *via* the COP adsorbent. The increase of ΔG value along with

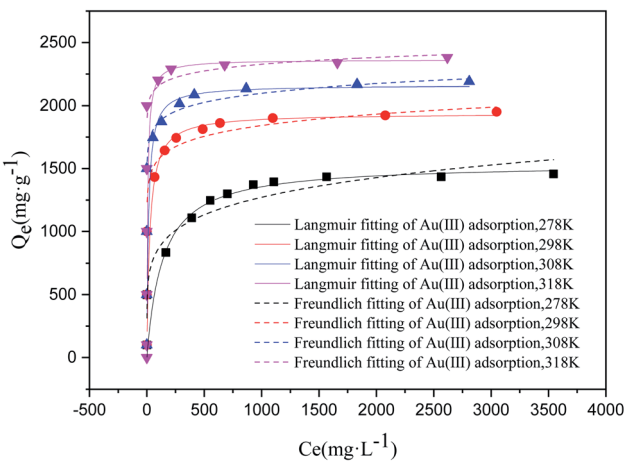

Fig. 4 The influence of concentration of Au^{3+} for adsorbing Au^{3+} over COP. Condition: pH of solution: 2.5; material: 10 mg; volume: 10 mL; adsorption time: 24 h.

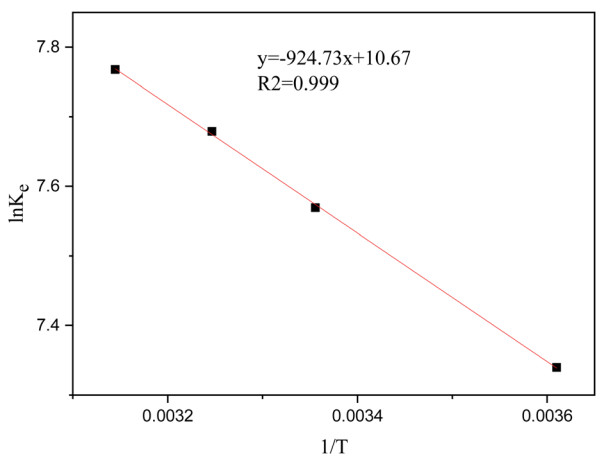

Fig. 5 The influence of temperature for adsorbing Au^{3+} over COP. Condition adsorption time: 24 h; pH of solution: 2.5; material: 10 mg; volume: 10 mL; concentration of Au(III): 3000 mg L^{-1}.

Table 3 Thermodynamics parameters of adsorbing Au^{3+} over COP

T (K)	K_e	ΔG (kJ mol^{-1})	ΔH (kJ mol^{-1})	ΔS (kJ mol^{-1} K^{-1})
278	1531.48	−16.97	7.69	88.71
298	1914.13	−18.74		
308	2116.82	−19.63		
318	2326.21	−20.52		

raising the temperature indicates the feasibility of adsorption. ΔS represents the randomness of the adsorption system. The ΔH value indicates that the adsorption process over COP adsorbent is endothermic, which is consistent with the batch adsorption experiment. On the basis of the third law of thermodynamics, $\Delta S > 0$ is conducive to the spontaneous adsorption process. Consequently, it can be considered that the increase in system entropy drives the adsorption of Au^{3+}.

3.3 Mechanism study

To study the mechanism, XPS, XRD, FI-RT, TEM, and SEM are used to analyze COP and Au-COP, respectively. The SEM image (Fig. 6a) shows that some attachments exist on the surface of the COP after adsorption, relative to that before adsorption (Fig. 1c). Except for C, N, and O, Au and Cl are detected in the elemental map of COP adsorbed by Au (Fig. 7b–e). Simultaneously, due to the porous material's porosity, Au and Cl are uniform distribution which can be seen from the obtained electron microscope image. The dense arrangement of nanoparticles can also be seen in the TEM images (Fig. 6b). PXRD is used to study the structure of the COP adsorbent further. As shown in Fig. 6c, the diffraction peaks at 38.16, 44.34, 64.56, 77.5, and 81.7 can be observed clearly, corresponding to the lattice planes of gold (111), (200), (220), (311), and (222), respectively.[11,13,24,25] Fig. 6d shows the Fourier transform infrared spectrum of COP after Au^{3+} treatment. The peak of N–H Tensile vibration on the material moved from 3379.7 cm^{-1} to 3342.5 cm^{-1} and 3223.2 cm^{-1}. The peak of C–NH stretching vibration moved from 1270.96 cm^{-1} to 1387.02 cm^{-1} after the adsorption of Au^{3+}. Besides, a larger concentration of Au^{3+} enhance the reduction process of C–NH, which means that Au^{3+} could reduce to Au(0) at the cost of amino. As shown in Fig. 1b, an N–H stretching vibration peak at 3342.5 cm^{-1} is observed in infrared spectrum for this material.[15] The peak located at 1624 cm^{-1} belongs to C=O tensile vibration.[21] The peak at 1481.49 cm^{-1} is assigned to tensile vibration of C=C bond, manifesting that the C=C bond resides in the material. The peak at 1270.92 cm^{-1} is connected to the tensile vibration of C–N bond, meaning that the C–N bond remains in the material.[21]

The valence states of adsorbed substances are analyzed by photoelectron spectroscopy. The measured XPS spectrum

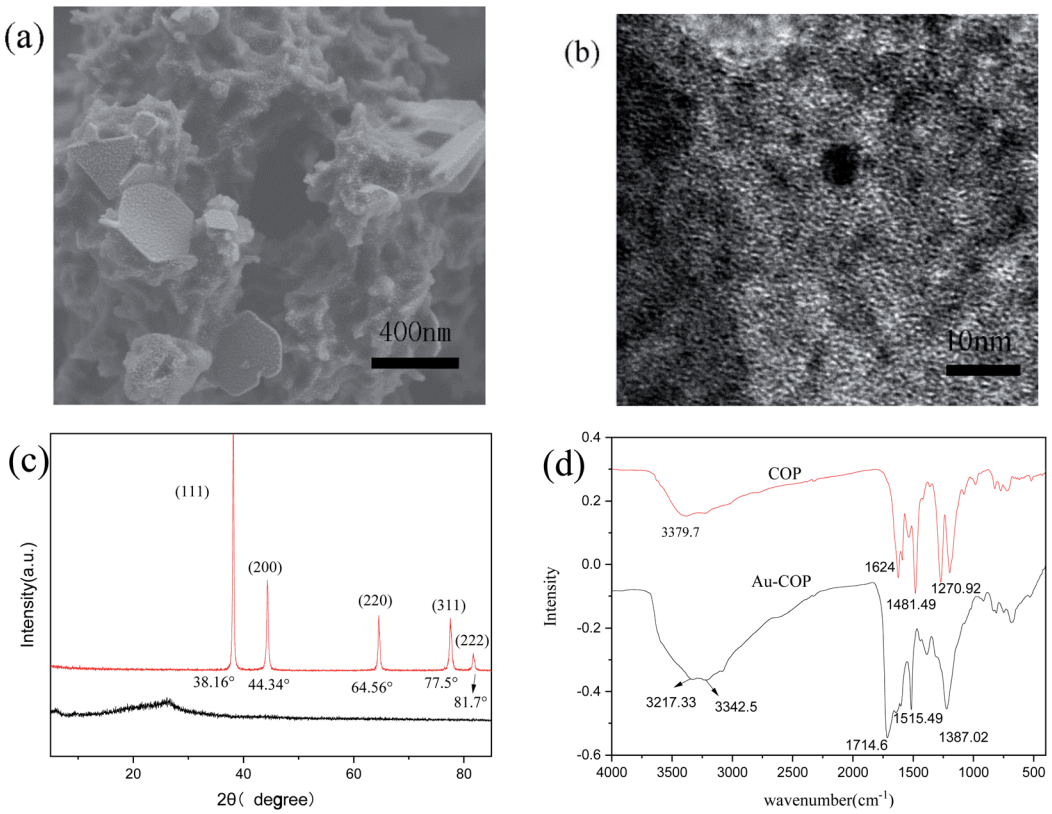

Fig. 6 The structure characterization of Au-COP. (a) SEM picture of Au-COP; (b) TEM picture of Au-COP; (c) PXRD spectrum before and after adsorption of Au^{3+} by COP; (d) FTIR spectra of COP before and after adsorption of Au^{3+}.

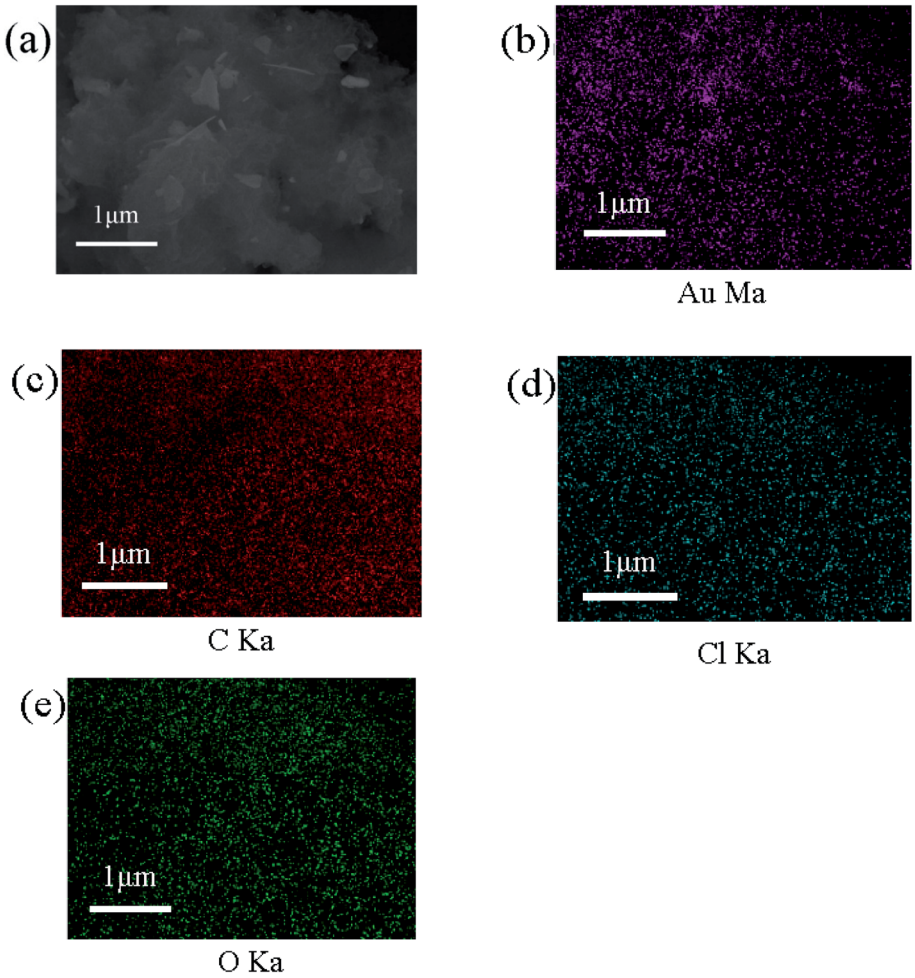

Fig. 7 The EDS and element distribution image of COP after adsorbing Au^{3+}. (a) EDS image of COP after adsorbing Au^{3+}; (b)–(e) element distribution of Au, C, Cl, O of COP after adsorbing Au^{3+}.

(Fig. 8a) indicates that the original material consists of C, N, and O, and new Cl and Au peaks appear after adsorption. The high-resolution spectrum of Au 4f is shown in (Fig. 8b). Two evident peaks are observed at 83.09 eV and 86.82 eV, which is assigned to Au(0). Two peaks are observed at 84.1 eV, and 88.02 eV is attributed to Au^{3+}. After adsorption, the relative amount of Au^{3+} decreased, and the relative amount of Au(0) increased, indicating that a part of Au^{3+} is reduced to form Au(0). Moreover, a peak appears in N 1s spectrum (Fig. 8c) of the original material, which may be due to the carbon C–NH at 398 eV.[26] Two peaks are detected in N 1s spectrum of the adsorbed Au^{3+} material. One is assigned to C–NH significantly reduced, and the other may have resulted from N–Au. The deconvolution C 1s spectrum (Fig. 8d) of the material adsorbing Au^{3+} is compared with the convolution C 1s spectrum of the initial material. It is found that there is one more peak, which might be C–Cl. It can be proved by the scanning electron microscope that Cl ion appeared after adsorption.

To further study the mechanism, dimethylamino phenyl propenone (1 eq.) is synthesized by nucleophilic substitution with aniline (1 eq.) and 10% *p*-toluenesulfonic acid in toluene. The dilute ketone and gold solution are mixed in the ratio of 1 : 1. There is an oxidation–reduction reaction in the adsorption process. The structure of Fig. 9 is obtained by single-crystal diffraction.

The results show that the adsorbing Au^{3+} process is mainly resulted from the reducibility of COP, not from the coordination interaction of COP. This result indicates that the COP adsorbent material possesses weak coordination ability to metal ions but unique reducing ability.

3.4 Selectivity study

In secondary recycling resources, Au always coexists with other metals, such as Co, Ni, Cu, and Fe. Obviously, the adsorbent's selectivity to Au is of great significance in the secondary recovery of resources. The effect of other metal ions on adsorption property of Au^{3+} over COP is studied. The COP adsorbent are added into the mixed solution of Au^{3+} (800 mg L^{-1}), Fe^{3+} (800 mg L^{-1}), Co^{2+} (800 mg L^{-1}), Ni^{2+} (800 mg L^{-1}) and Cu^{2+} (800 mg L^{-1}) to simulate secondary recovery. The adsorption capacity of Fe^{3+}, Co^{2+}, and Ni^{2+} over COP can be almost

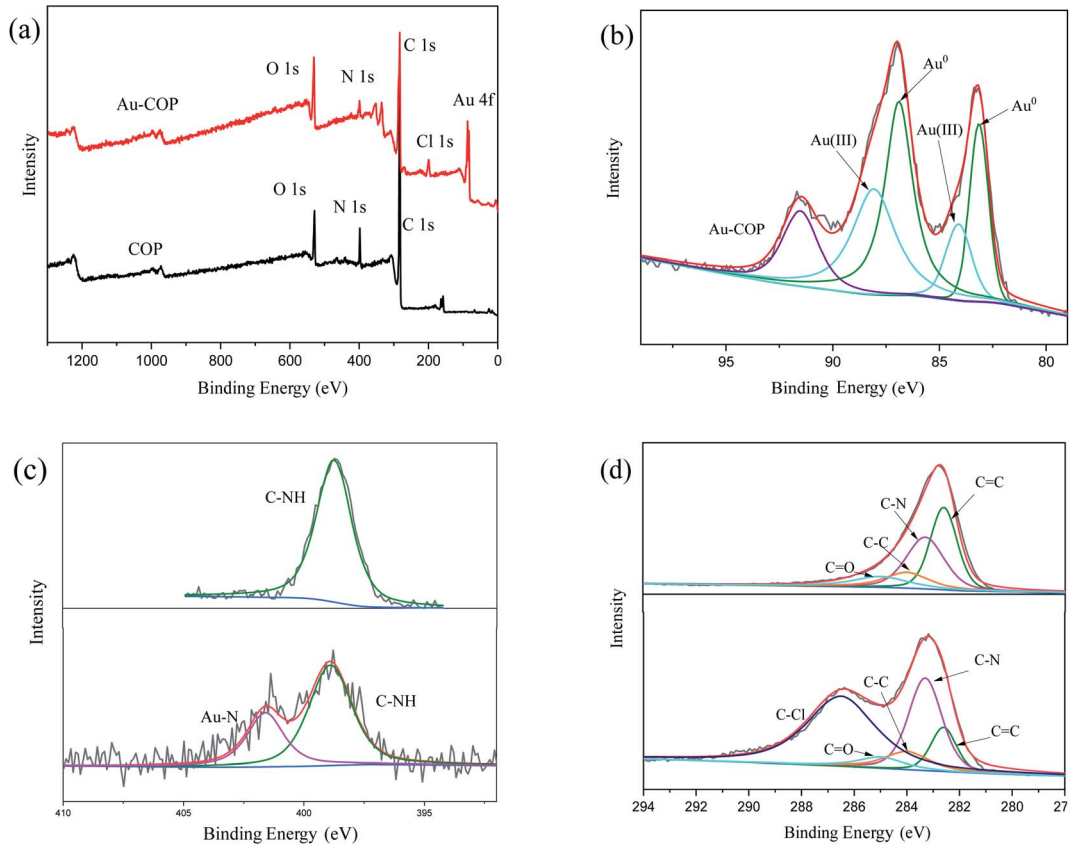

Fig. 8 The XPS spectra of COP before and after adsorbing Au^{3+}. (a) XPS spectra of COP before and after adsorbing Au^{3+}; (b) Au 4f spectra of COP after adsorbing Au^{3+}; (c) N 1s spectra of COP before and after adsorbing Au^{3+}; (d) C 1s spectra of COP before and after adsorbing Au^{3+}.

neglectable while that of Au^{3+} is still enormous, as shown in Fig. 10. This result indicates that the Fe^{3+}, Co^{2+}, and Ni^{2+} ions have little effect for adsorbing Au^{3+} over COP. Besides, the adsorption capacity of Cu^{2+} ion over COP could reach 18.7%, but it still makes no difference for the adsorption of Au^{3+}. Therefore, the selectivity of adsorbents for Au is of great significance in recovering Au from secondary recovery resources. In addition, the adsorption capacity of the same type of adsorbent to Au^{3+} is compared in Table 4. The results show that this polymer is a good adsorption capacity for Au^{3+}, which than some reported adsorbents.

3.5 Renewability study

In the practical application of industry, the recyclability of adsorbent is very important, which has great economic significance. In this study, after adsorption with 1000 mg L^{-1}

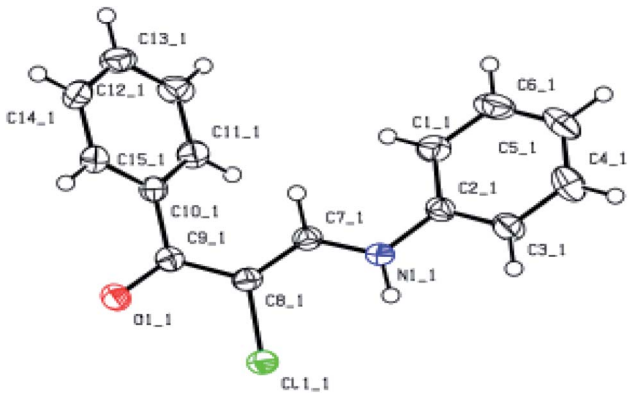

Fig. 9 X-ray crystal structure of COP after adsorbing Au^{3+}.

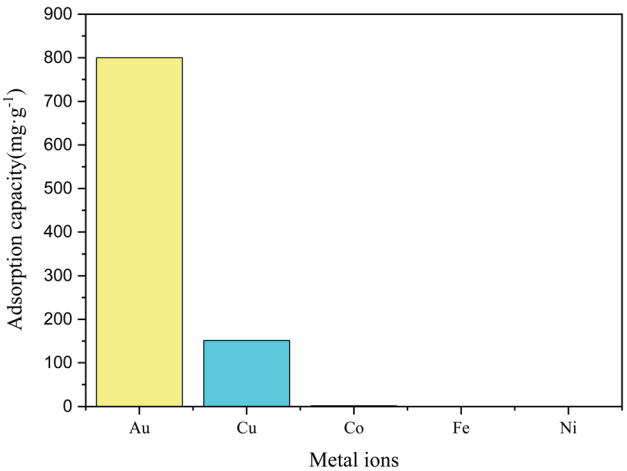

Fig. 10 The adsorptive selectivity of COP for various metal ions.

Table 4 Comparison of various polymers for adsorbing Au(III)

Adsorbents	q_{max} (mg g^{-1})	Ref.
Enaminone polymer	1945	This work
UiO-66-NH_2	650	27
JNU-1	1124	28
TRF	1432	29
BT-SiO_2	642.0	30
PANF-ATL	130.6	31

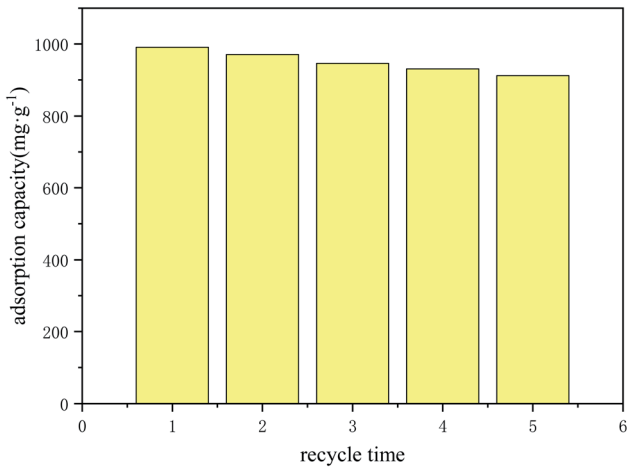

Fig. 11 The reusability of COP. Condition: adsorption time: 24 h; pH of solution: 2.5; material: 10 mg; volume: 10 mL; concentration of Au(III): 1000 mg L^{-1}.

Au^{3+} solution, the gold adsorbed COP is eluted with 10 mL acidified thiourea in a 50 mL centrifuge tube for 24 h, and then washes with deionized water three times. After that, the updated COP is used to the subsequent adsorption test. As shown in Fig. 11, after five cycles, the adsorption capacity of COP do not decrease significantly, indicating that COP has excellent reusability.

4. Conclusion

In this paper, a covalent organic polymer of enaminone is synthesized effectively and employed as adsorbent to adsorb Au^{3+} ion from an aqueous solution. Batch adsorption experiments and surface analysis were studied and the mechanism was suggested. These experimental results manifested that the adsorption capacity of Au^{3+} over the COP adsorbent increase along with the decreasing pH of the solution. A pseudo-second-order kinetic model provided a good explanation for the adsorption kinetics of Au^{3+}. Meanwhile, the adsorption isotherm was in accord with the Langmuir equation. As a result, the adsorption capacity could reach up to 1945 mg g^{-1} at 298 K. Thermodynamic calculations demonstrated that the Au^{3+} adsorption process was endothermic and spontaneous, which was resulted from the increasing of the randomness of the system. The mechanism study manifested that the excellent adsorption performance of the COP adsorbent was mainly attributed to the good reducibility rather than the coordination interaction of COP. Moreover, The COP adsorbent exhibited excellent adsorptive selectivity and reusability of Au^{3+} with the existence of interfering ions. It was feasible to recover gold from mixed ion recovered solution.

Conflicts of interest

The authors declare no competing financial interest.

Acknowledgements

This work was supported by the National Natural Science Foundation of China (No. U20A20268 and 51974122), and the Scientific Research Fund of Hunan Provincial Education Department (No. 19A209 and 20B258).

References

1 R. Ciriminna, E. Falletta, C. Della Pina, J. H. Teles and M. Pagliaro, *Angew. Chem., Int. Ed.*, 2016, **55**, 14210–14217.
2 M. Rigoulet, O. Thillaye du Boullay, A. Amgoune and D. Bourissou, *Angew. Chem., Int. Ed.*, 2020, **59**, 16625–16630.
3 C. Praveen, *Catal. Rev.*, 2019, **61**, 406–446.
4 Y. Huang, P. Huang and J. Lin, *Small Methods*, 2019, **3**, 1800394.
5 J. Lou-Franco, B. Das, C. Elliott and C. Cao, *Nano-Micro Lett.*, 2020, **13**, 2311–6706.
6 M. Gorbunova, V. Apyari, S. Dmitrienko and Y. Zolotov, *TrAC, Trends Anal. Chem.*, 2020, **130**, 115974.
7 W. Wei, F. Bai and H. Fan, *Angew. Chem., Int. Ed.*, 2019, **58**, 11956–11966.
8 I. Korolev, P. Altınkaya, P. Halli, P.-M. Hannula, K. Yliniemi and M. Lundström, *J. Cleaner Prod.*, 2018, **186**, 840–850.
9 W. Zhang, L. Wu, X. Han, L. Yao, S. Zhao, J. Sun, Y. Xu, J. Li and C. Xiong, *J. Hazard. Mater.*, 2019, **378**, 120674.
10 X. Huang, Y. Wang, X. Liao and B. Shi, *J. Hazard. Mater.*, 2010, **183**, 793–798.
11 S. I. Park, I. S. Kwak, S. W. Won and Y. S. Yun, *J. Hazard. Mater.*, 2013, **15**, 211–218.
12 W. Xu, X. Mo, S. Zhou, P. Zhang, B. Xiong, Y. Liu, Y. Huang, H. Li and K. Tang, *J. Hazard. Mater.*, 2019, **380**, 120844.
13 I. S. Kwak, M. A. Bae, S. W. Won, J. Mao, K. Sneha, J. Park, M. Sathishkumar and Y.-S. Yun, *Chem. Eng. J.*, 2010, **165**, 440–446.
14 P. J. Tauetsile, E. A. Oraby and J. J. Eksteen, *Hydrometallurgy*, 2018, **178**, 195–201.
15 Z. Chang, F. Li, X. Qi, B. Jiang, J. Kou and C. Sun, *J. Hazard. Mater.*, 2020, **391**, 122175.
16 Z. Dong, T. Jiang, B. Xu, Y. Yang and Q. Li, *J. Cleaner Prod.*, 2019, **229**, 387–398.
17 B. Xu, K. Li, Z. Dong, Y. Yang, Q. Li, X. Liu and T. Jiang, *J. Cleaner Prod.*, 2019, **233**, 1475–1485.
18 D. L. C. Wang and W. Lin, *J. Am. Chem. Soc.*, 2013, **135**(36), 13222.

19 Y. Cui, B. Li, H. He, W. Zhou, B. Chen and G. Qian, *Acc. Chem. Res.*, 2016, **49**, 483–493.
20 X. Chen, Y. Xiang, L. Xu and G. Liu, *J. Hazard. Mater.*, 2020, **397**, 122812.
21 C. Wang, W. Gao, N. Liu, Y. Xin, X. Liu, X. Wang, Y. Tian, X. Chen and B. Hou, *Corros. Sci.*, 2020, **176**, 108920.
22 G. L. Chen Wang, J. Zhao, S. Wang and L. Zhang, *Chem. Eng. J.*, 2020, **388**, 124221.
23 E. C. Lima, A. Hosseini-Bandegharaei, J. C. Moreno-Piraján and I. Anastopoulos, *J. Mol. Liq.*, 2018, **273**, 425–434.
24 C.-H. Yen, H.-L. Lien, J.-S. Chung and H.-D. Yeh, *J. Hazard. Mater.*, 2017, **322**, 215–222.
25 J. Zhao, C. Wang, S. Wang, L. Zhang and B. Zhang, *J. Cleaner Prod.*, 2019, **236**, 117605.
26 H. L. Qian, F. L. Meng, C. X. Yang and X. P. Yan, *Angew. Chem., Int. Ed.*, 2020, **59**, 17607–17613.
27 Z. Chang, X. Qi, B. Jiang, J. Kou and C. Sun, *J. Hazard. Mater.*, 2019, **391**, 122175.
28 H. L Qian, F. L. Meng, C. X. Yang and X. P. Yan, *Angew. Chem., Int. Ed.*, 2020, **59**, 17607–17613.
29 X. Chen, L. Xu and G. Liu, *J. Hazard. Mater.*, 2020, **397**, 122812.
30 X. Huang, X. Liaoa and B. Shi, *J. Hazard. Mater.*, 2010, **183**, 793–798.
31 W. Zhang, X. Han, L. Yao, S. Zhao, J. Sun, Y. Xu, J. Li and C. Xiong, *J. Hazard. Mater.*, 2019, **378**, 120674.